Catalysis
Science & Technology

Dynamic Article Links

Cite this: *Catal. Sci. Technol.*, 2012, **2**, 316–323

www.rsc.org/catalysis

PAPER

Speciation of $Pd(OAc)_2$ in ligandless Suzuki–Miyaura reactions†

Luis A. Adrio,[a] Bao N. Nguyen,[a] Gemma Guilera,‡[b] Andrew G. Livingston[c] and King Kuok (Mimi) Hii*[a]

Received 30th June 2011, Accepted 16th August 2011
DOI: 10.1039/c1cy00241d

Generation of catalytically active Pd(0) species from $Pd(OAc)_2$ has been examined, in the context of Suzuki–Miyaura reactions involving substitution of aryl bromides under aerobic and ambient conditions. Using a combination of spectroscopic, microscopic and kinetic measurements, the role of each reaction component is delineated in the speciation of the palladium species. Among the key findings are the effects of O_2, H_2O and inorganic base, and implications for catalytic activity.

1. Introduction

The discovery of the Suzuki–Miyaura (SM) cross-coupling reaction is undoubtedly one of the important landmarks of organic chemistry for the 20th century. Providing a reliable protocol for the formation of aryl–aryl bonds, it has stimulated great progress in modern material[1–4] and medicinal chemistry.[5–11] Accordingly, there is sustained interest in developing Pd catalysts that can offer the requisite reactivity with high TON and TOF. To this end, a number of ligands were developed, which can generate highly active catalysts with wider scope,[12–14] allowing these processes to be viable on an industrial scale.[15]

Conversely, there is significant interest in the development of 'ligandless' protocols.[16–23] Although the scope of the catalytic system is presently limited to aryl iodides, bromides and certain activated chlorides, these are very often adequate for most transformations, and offer a practical alternative to ligand-promoted reactions, as they can be performed aerobically and bypasses issues related with cost and removal of the ligand.

Very often, $Pd(OAc)_2$ is employed as a catalyst precursor in these reactions, which is reduced *in situ* to form catalytically active Pd(0) species, in molecular, colloidal and/or nanoparticle forms, that can catalyse cross-coupling reactions at ambient temperature.[17,24] Further aggregation of these species to form larger particles deactivates the catalyst, eventually leading to the deposition of Pd black (Fig. 1). The process can be dependent upon the reaction medium, oxygen, moisture and additives/stabilizers.

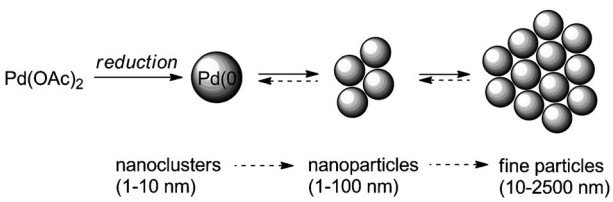

Fig. 1 Process of catalyst activation and deactivation by aggregation.

A plethora of additives/stabilizers has been reported for 'ligandless' SM reactions,[21,23,25–28] but this is not always necessary; we[29] and others[17,24] have shown that $Pd(OAc)_2$ alone is sufficient for high turnovers. Notably, these reactions occur in protic solvents such as alcohols, ethylene glycol derivatives, or mixtures of water with organic solvents. Previously, the formation of Pd nanoparticles from $Pd(OAc)_2$ under Suzuki coupling reaction conditions was reported to be promoted by O_2 in PEG-400.[27,28] More recently, $PdCl_2$ can also be activated towards catalysis in an aqueous media under an aerobic atmosphere.[30] In these papers, the beneficial effects of O_2 and H_2O were illustrated by the comparison of isolated yields, rather than kinetic profiles, and it was not clear how these promoters exert a beneficial effect for catalysis. In the present work, we will delineate the role of each of the reacting components in catalyst activation, stability and eventual deactivation.

2. Experimental

2.1 Materials

All chemical reagents were procured commercially and used as received unless otherwise indicated. Anhydrous solvents were dried in a purification system by passing through columns of

[a] *Department of Chemistry, Imperial College London, Exhibition Road, South Kensington, London SW7 2AZ, UK. E-mail: mimi.hii@imperial.ac.uk; Fax: +44-20-7594 5804; Tel: +44-20-7594 1142*
[b] *European Synchrotron Radiation Facility (ESRF), P. O. Box 220, 38043 Grenoble Cedex, France*
[c] *Department of Chemical Engineering and Chemical Technology, Imperial College London, UK*

† Electronic supplementary information (ESI) available: Details of UV-vis stopped-flow and EXAFS experiments, and associated data fitting. See DOI: 10.1039/c1cy00241d

‡ Dr Gemma Guilera, current affiliation: ALBA Synchrotron Light Source, Experiments Division, Crta. BP 1413 Km 3.3, 08290 Cerdanyola del Vallès, Barcelona, Spain.

activated molecular sieves under N_2. $Pd(OAc)_2$ (Pd-111) was obtained from Johnson Matthey plc through an academic loan scheme.

2.2 Experimental methods

Catalytic reactions were monitored by recording ^1H (400 MHz) and ^{19}F (376 MHz) NMR spectra of reaction mixtures in $CDCl_3$ on Bruker Avance-400 spectrometers. High-resolution TEM images were recorded using a JEOL 2010 instrument, fitted with an analytical pole-piece (resolution 0.23 nm, +/− 30° tilt), in bright field mode. Stopped-flow experiments were performed using a Bio-Logic SFM-300 multi-mixer fitted with a MPS-52 syringe controller and Bio-Kine32 software, and equipped with a TC-100 quartz cuvette (10 × 1.5 mm, transparency between 185–2500 nm), with a total volume of 45 μL. UV-Vis spectra were measured using a deuterium tungsten light source and a multiwavelength J&M TIDAS diode array for spectra collection with an integration time of 15 ms. EXAFS experiments were conducted at the dispersive undulator beamline ID24 of the ESRF, Grenoble, France, operating at an average current of *ca.* 90 mA. The absorption measurements were performed using a Si (311) polychromator in the Bragg configuration. EXAFS spectra at the Pd K-edge (24.35 keV) were collected in transmission mode with 1 s (1 ms × 1000 accumulations) resolution. An FReLoN2k (Fast Readout Low Noise) CCD camera working in kinetic mode was used to collect the data.[31] A Pd reference foil was measured regularly to provide the energy calibration for the spectra and was used to determine the multiple electron reduction factor to be employed for the EXAFS analysis of the samples (S_0^2 = 0.78). The EXAFS data were background subtracted and normalised following standard procedures using the software package Viper v. 10.1 for Windows.[32] Radial distribution functions were obtained by Fourier transformation of the k^2-weighted EXAFS functions. Amplitudes and phases for single and multiple scattering contributions to the EXAFS signal have been obtained by applying the FEFF7 code to different crystallographic model compounds. The fitting procedure has been performed in back Fourier k space and crossed-checked on R space. High-resolution TEM images were recorded using a JEOL 2010 instrument. ICP-OES (Pd, P) and combustion analyses (C, H) were carried out by a commercial provider.

2.2.1 Catalytic reaction with the catalyst generated *in situ* (Fig. 2). A reaction vial fitted with a rubber septa was charged with 1-bromo-4-chlorobenzene **1** (189.9 mg, 1 mmol, 1 eq.), (4-fluorophenyl)boronic acid **2** (154 mg, 1.1 mmol, 1.1 eq.), anhydrous K_3PO_4 (424.5 mg, 2 mmol, 2 eq.) and $Pd(OAc)_2$ (2.3 mg, 0.01 mmol, 0.01 eq., 1 mol%). A magnetic stir bar was added, and the flask was sealed and purged with N_2 or O_2. 6 mL of a 2 : 1 v/v mixture of THF–H_2O (degassed for reactions under N_2) was then added, and the resultant mixture was stirred at room temperature for up to 2 h. During this period, aliquots of the reaction mixture (0.2 mL) were extracted and diluted with CH_2Cl_2 (1.5 mL), dried over $MgSO_4$, filtered through cotton wool, and evaporated. The residue was dissolved in $CDCl_3$ and subjected to ^1H NMR and ^{19}F NMR analyses. Product conversion was determined by ^1H NMR integration.

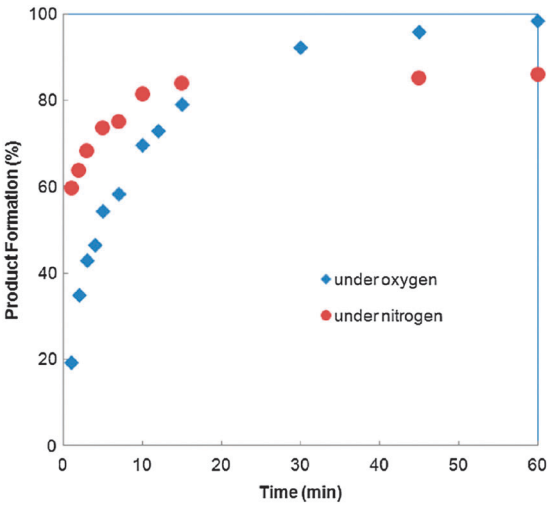

Fig. 2 Effect of O_2 on the reaction (at 1 mol% catalyst loading).

2.2.2 Catalytic reaction with the prepared catalyst (Fig. 3 and 4). A stock solution (Solution A) of the catalyst precursor was prepared by dissolving $Pd(OAc)_2$ (1.1 mg) in the appropriate reaction medium (1 mL). 100 μL of A (containing 0.05 mol% of Pd) was injected into a mixture of 1-bromo-4-chlorobenzene (189.9 mg, 1 mmol, 1 eq.), (4-fluorophenyl)-boronic acid (154 mg, 1.1 mmol, 1.1 eq.), anhydrous K_3PO_4 (424.5 mg, 2 mmol, 2 eq.) in THF–H_2O (2 : 1 v/v, 5.9 mL) (Solution B). A magnetic stir bar was added, and the resultant mixture was stirred at room temperature. Periodically, aliquots of the reaction mixture (0.2 mL) were extracted and diluted with CH_2Cl_2 (1 mL) and H_2O (1 mL), dried over $MgSO_4$, filtered through cotton wool, and evaporated. The residue was dissolved in $CDCl_3$ and subjected to ^1H NMR and ^{19}F NMR analyses. Product conversion was determined by ^1H NMR integration.

2.2.3 Homocoupling of 4-fluorophenylboronic acid (Scheme 2). A reaction vial was charged with a stir bar, $Pd(OAc)_2$ (3.3 mg, 0.015 mmol), (4-fluorophenyl)boronic acid (140 mg, 1 mmol), and K_2CO_3 (172.5 mg, 1.25 mmol.) or anhydrous K_3PO_4 (424.5 mg, 2 mmol.). A mixture of acetone–water (1 : 1 v/v, 4 mL) or THF–water (2 : 1 v/v, 4 mL) was added. The reaction vial was then fitted with a rubber septum to which a balloon of O_2 was attached, and the mixture was stirred at room temperature for 16 h. The solvent was then evaporated,

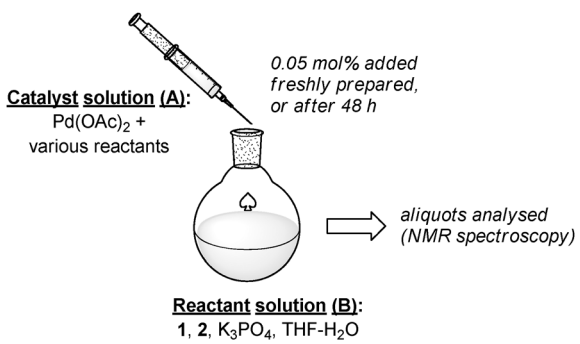

Fig. 3 Assessment of catalytic performance of $Pd(OAc)_2$.

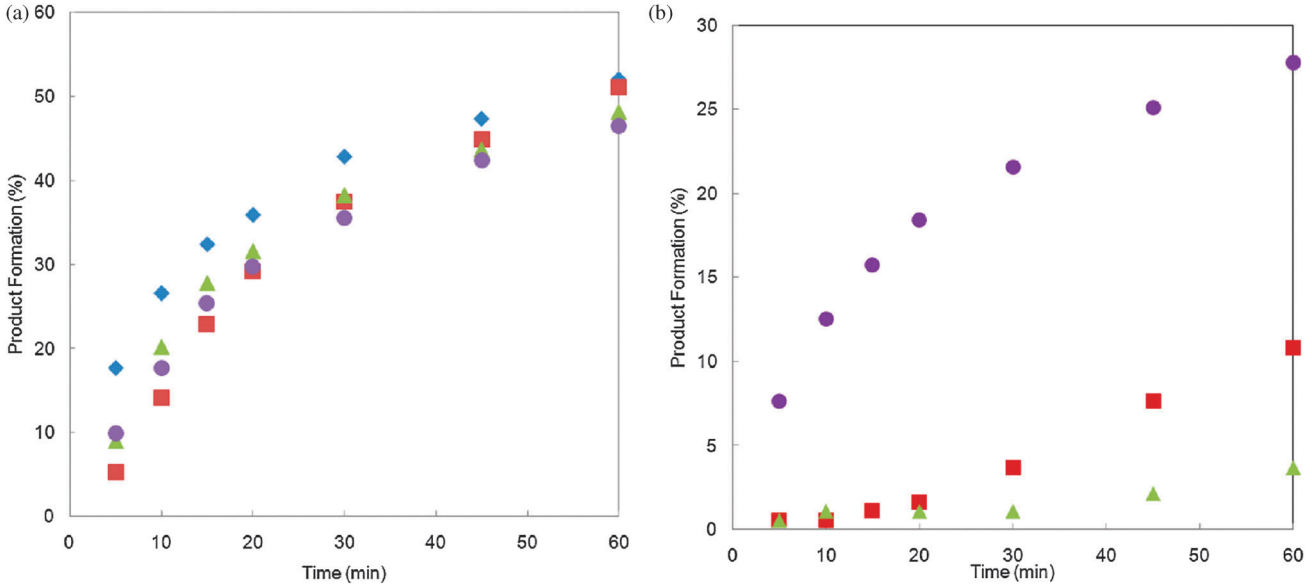

Fig. 4 Catalytic activities of solutions A prepared in: THF (◆), THF–H_2O (■), K_3PO_4, in H_2O only (▲) and arylboronic acid (**2**), THF (●). Effective catalyst loading = 0.05 mol%. Reaction progress with: (a) freshly prepared solution (left), and (b) after standing at room temperature for 48 h (right).

and the residue was subjected to ^1H and ^{19}F NMR analyses. Product conversion was determined by ^1H NMR integration.

2.3 Stopped-flow experiments

Prior to the experiment, the stopped-flow system was purged with the solvent three times. Solutions of $Pd_3(OAc)_6$ (8.9 mM) and arylboronic acid (17.8 mM) were prepared under N_2 and anhydrous conditions using Schlenk techniques unless otherwise specified. UV-vis spectra were collected every 0.5 s between 200–700 nm, observing absorbance peaks due to $Pd_3(OAc)_6$ (300 nm), biaryl (λ_{max} = 300 nm) and Pd–Pd formation (450 nm). The kinetic model was fitted using Berkeley Madonna™ programme (Modelling and Analysis of Dynamic Systems).

3. Results and discussion

3.1 Effect of O_2

The reaction between 4-chlorobromobenzene (**1**) and 4-fluorophenylboronic acid (**2**) in a mixture of THF–H_2O was chosen as the model system for our initial study (Scheme 1), where the C–C bond formation occurs specifically at the C–Br position.

Using 1 mol% of $Pd(OAc)_2$ as the catalyst precursor, reactions were conducted under an atmosphere of O_2 or N_2 (Fig. 2). No induction period was observed in either of these reactions, signifying that the generation of an active catalyst is extremely rapid. Significantly, the results clearly indicated that the role of O_2 is to prevent catalyst deactivation: under an inert N_2 atmosphere, very fast catalytic turnovers were observed initially, reaching >80% conversion within 10 min, but the reaction was curtailed at *ca.* 86% conversion. In contrast, the reaction performed under O_2 has a slower initial rate, but turnover was maintained until it reached completion within 60 min. Thus, the presence of O_2 suppresses both catalyst activation and deactivation processes, affording a higher overall conversion.

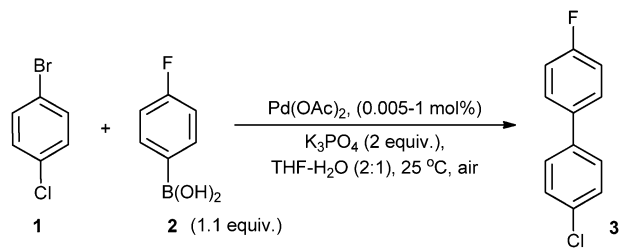

Scheme 1 Model SM reaction used in this work.

3.2 Homo- *vs.* cross-coupling

Homocoupling of the arylboronic acid is also reported to be catalysed by ligandless $Pd(OAc)_2$, facilitated by moisture and air,[33] but it was not a significant process in any of the experiments conducted in the present study.[34] This was investigated by exposing arylboronic acid **2** to O_2 and 3 mol% of $Pd(OAc)_2$ under reaction conditions prescribed for homo-[33] and cross-[29] coupling conditions, I and II, respectively (Scheme 2). The reaction conducted using K_2CO_3 proceeded with quantitative conversion of **2** to biaryl **4**, whereas only 32% of the homocoupled product was obtained when K_3PO_4 was employed. Thus, the choice of an inorganic base and a solvent system has a profound effect on the

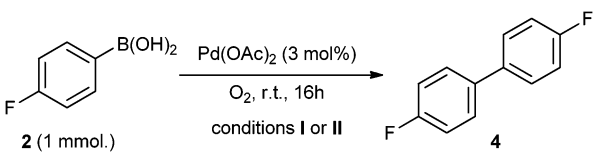

Scheme 2 Homocoupling of arylboronic acid **2** by $Pd(OAc)_2$: Conditions **I**: K_2CO_3, acetone–water (1 : 1), >99% conversion. Conditions **II**: K_3PO_4, THF–water (2 : 1), 32% conversion.

partition of the reaction pathway—*i.e.* when K_3PO_4 is employed as a base, the homocoupling process can be considered as non-competitive.

3.3 Catalyst activation/stability

To interrogate the effect of other reaction components on catalyst stability/activation, catalytic loading was lowered to 0.05 mol% to ensure observable and comparable rates.[35] A stock solution of $Pd(OAc)_2$ was prepared in THF under aerobic conditions, to which individual components of the reaction (water, base or aryl boronic acid) was added (Solution A). This was injected into a mixture of reactants (aryl bromide, aryl boronic acid and base) in a 2 : 1 mixture of THF–H_2O[36] (Solution B). The reaction progress was monitored by ^1H NMR analysis of extracted reaction aliquots (Fig. 3). The catalyst activity of solution A was evaluated when freshly prepared, and reassessed after it has been 'aged' for 48 h.

Freshly prepared solutions A (used within 5 minutes of preparation) showed similar temporal profiles within the first 60 min of the reaction, signifying that the amount of the active catalyst generated is little affected by the presence of water, inorganic base and arylboronic acid (Fig. 4a). After 48 h, the $Pd(OAc)_2$ precursor in solutions A evolved into separate species, reflected in different observed reaction profiles (Fig. 4b); while the solution containing arylboronic acid initiated catalytic activity instantaneously, notable induction periods were observed when the precursor was left exposed to water or K_3PO_4.

3.4 Effect of a base (K_3PO_4)

Tripotassium phosphate (K_3PO_4) is a general inorganic base used in many ligandless protocols for SM[29] and also Heck[37] reactions. It is important to note that although THF and water are miscible to a certain extent, the dissolution of the reactants causes them to separate, such that the reaction occurs in a biphasic solution. By adding K_3PO_4 to a solution of $Pd(OAc)_2$ in aqueous THF,[38] a light-orange solid slowly precipitates as more K_3PO_4 is added, signifying a formation of a new compound (Fig. 5), which is water-soluble.[39] Elemental analyses of the precipitate revealed a Pd : P : C ratio of 4 : 1 : 1,[40] suggesting the formation of a complex salt through an anion-exchange process, likely to be a network of bridged oxo-/hydroxopalladium units, interspersed by phosphate and acetate anions.

3.5 Solution structure of $Pd(OAc)_2$

Due to the ambidentate nature of the acetate anion, $Pd(OAc)_2$ can exist in several aggregated forms (Fig. 6). While trimeric[41] (**5**) and polymeric[42] structures have both been found in the solid state, its solution structure remains controversial. Early independent studies by Wilkinson and Pandey suggested, by molecular weight measurements, that it exists as a trimer (**5**) in benzene[43] and acetic acid[44] at ambient temperatures. A much later study by Stoyanov using infrared spectroscopy, however, suggested the existence of an equilibrium process between **5** and a linear dimer (**6**) in chloroform–acetic acid.[45] A few years later, the monomeric form of $Pd(OAc)_2$ (**7**) was detected in *N*-methyl-2-pyrrolidinone (NMP) by Evans *et al.*, by examining the EXAFS at the Pd K-edge.[46] This was closely followed by a ^1H NMR study by Cotton and co-workers, which showed that the trimeric structure (**1**) is largely retained in methanol, chloroform and benzene.[47]

The dipole moment or dielectric constant of a solvent is frequently invoked to describe its polarity, although the two properties are intrinsically different. This can be demonstrated by comparing methanol with NMP, which have markedly different dipole moments, yet very similar dielectric constants (Table 1). Conversely, water has a similar dipole moment to THF, but dramatically different dielectric constants.

An initial assessment of results of previous studies with the values presented in Table 1 appears to suggest a greater correlation between the nuclearity of the $Pd(OAc)_2$ and the dipole moment of the solvent in which it is dissolved. With this in mind, the structure of $Pd(OAc)_2$ was examined using Extended X-ray Absorption Fine Structure (EXAFS) spectroscopy at the Pd K-edge (24.35 keV). EXAFS spectra were recorded of the sample as a solid, and also as solutions in toluene and DMF, chosen for their very different polarities.

The data of the solid sample fit well with the crystallographic data reported for the trimeric structure. Due to the limited solubility of the palladium salt in toluene, solutions of a lower concentration (40 mM) were used compared to that

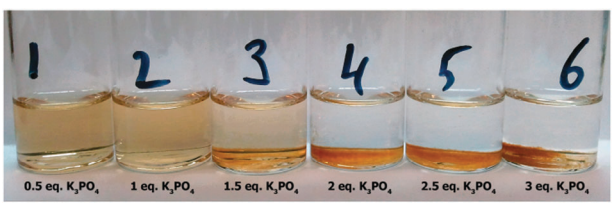

Fig. 5 Solutions containing $Pd(OAc)_2$ (0.5 mM) with varying amounts of K_3PO_4 in THF–H_2O (1 : 1).

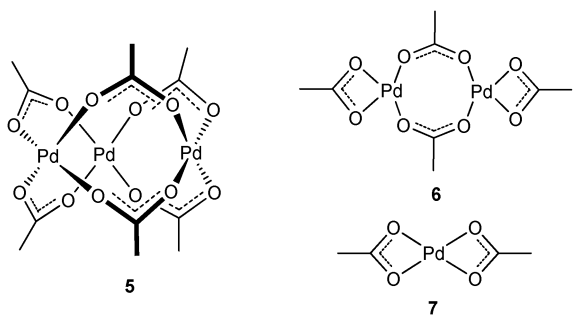

Fig. 6 Suggested structures of $Pd(OAc)_2$.

Table 1 Selected solvent properties[48]

Solvent	Dipole moment (D)	Dielectric constant
Benzene	0	2.28
Toluene	0.36	2.38
Chloroform	1.15	4.81
Acetic acid	1.68	6.15
THF	1.75	7.5
Methanol	2.87	32.7
N,*N*-Dimethylformamide	3.86	36.7
NMP	4.09	32.2
Water	1.85	80

Table 2 EXAFS analysis for $Pd(OAc)_2$ samples[a]

Sample	Neighbour	CN[b]	R/Å[c]	σ^2/Å^{-2}[d]	ΔE_0/eV[e]
Solid[f]	O	4.8(4)	2.016(6)	0.003(1)	−1.85(3)
R = 10.6%	C	4	2.954(6)	0.005	−4.85
	Pd	2.2(3)	3.106(4)	0.006(1)	−4.85
In toluene[g]	O	4.38(30)	2.018(6)	0.004(2)	0.18(2)
R = 15.4%	C	4	2.898(7)	0.005	−2.81
	Pd	0.65(40)	3.085(12)	0.006(2)	−2.81
In DMF[h]	O	4.03(15)	2.046(5)	0.005(1)	2.05(1)
R = 17.1%	C	4	2.895(7)	0.005	−0.95
	Pd	0.45(20)	3.134(29)	0.012	−0.95

[a] Parameters in italics were restricted in the fit (see Experimental). [b] Coordination number. [c] Interatomic distance. [d] Debye–Waller factor. [e] Energy variation in the Fermi level from theory. [f] 3.84 < k < 16.69; ΔR = 2.38 Å. [g] 3.84 < k < 11.58; ΔR = 2.07 Å. [h] 3.84 < k < 11.58; ΔR = 1.91 Å.

used previously in NMP (50 mM).[46] Structural parameters extracted from the refinement fits of the EXAFS signals are shown in Table 2. The fitted curves to the experimentally obtained EXAFS signals can be found in the ESI.†

Dissolution in toluene caused a significant reduction of the FT peak corresponding to the Pd–Pd distance (indicated by the dashed line, Fig. 7), concomitant with a decrease in the Pd–Pd coordination number, and the shortening of Pd–C contact; both these parameters reduced by switching the solvent from toluene to DMF (indicated by the blue line, Fig. 7). Interestingly, there is an observable lengthening of the Pd–O bond length in the order: solid < toluene solution < DMF solution. Additionally, the quality of the fits to **5**, although reasonable, worsens the same order. These observations suggest the existence of an equilibrium process between the trimer and other species. The data suggest that the presence of the dimeric structure (**6**) is unlikely to be significant. As well as being a poor fit with the experimental data, its Pd–Pd distance (2.38–2.58 Å) was also not observable in the FT spectrum.

Principal Component Analysis (PCA) was subsequently performed using linear combinations of monomeric and trimeric

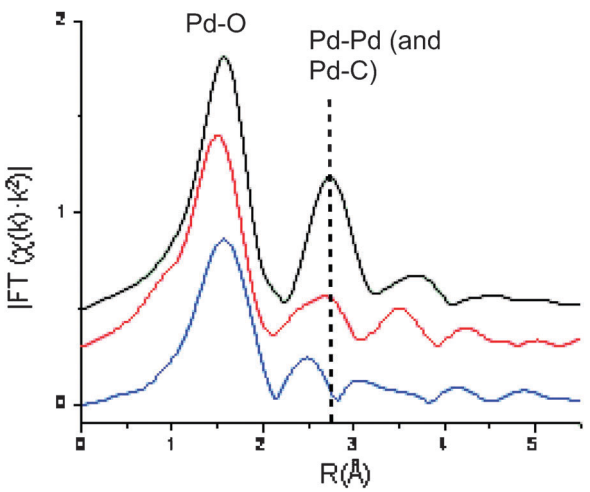

Fig. 7 Pd K-edge k^2-weighted FT modulus (uncorrected) of $Pd(OAc)_2$ in the solid state (black), and as 40 mM solutions in toluene (red) and DMF (blue). Pd–Pd distance is indicated by the vertical dashed line.

Table 3 Distribution of Pd species in solution (40 mM)

Solvent	Trimer, **5** (%)	Monomer, **7** (%)	Pd (particles/6) (%)
Toluene	71	21	2
DMF	56	42	8

Pd species, with or without the presence of a third component, which may be Pd particles or **6**. The result showed that the inclusion of a third component did not influence the global outcome of the analysis (Table 3), *i.e.* if a third species is present, it is beyond the detection limit of the technique (<8%). Some considerations upon this analysis can be found in the ESI.†

It is important to acknowledge that these experiments were conducted in an X-ray beam, where local heating cannot be ruled out. Nevertheless, it supports the ability of the $Pd(OAc)_2$ trimer **5** to dissociate to (primarily) monomers in solution, the degree of dissociation increases along with the dipole moment of the solvent, in the order: toluene (21%, 0.36 D) < DMF (42%, 3.86 D) < NMP (100%, 4.09 D); while earlier studies conducted in relatively less polar solvents (benzene, acetic acid and methanol, all <2.9 D) supported (predominantly) the trimeric structure.

3.6 Stability of $Pd(OAc)_2$ in the presence of water and arylboronic acid

The stability of the $Pd(OAc)_2$ precursor was found to be affected by water and arylboronic acid in the earlier part of this study (Fig. 4a and b). To assess these processes in detail, stopped-flow equipment coupled with a UV-spectrometer was used to examine the reaction between palladium(II) acetate with water and arylboronic acid. Using anhydrous THF as a solvent,[49] the trimeric structure **5** gives rise to a unique UV absorption peak at 300 nm, which is stable over a period of time. The addition of water triggers two consecutive processes: the first step gives rise to an intermediate species, which decays *via* a unimolecular process. The first of these processes is dependent upon $[H_2O]$, related by a first order relationship (Fig. 8). Subsequent curve fitting yielded values of 4.5×10^{-3} M^{-1} s^{-1} and 1.7×10^{-3} s^{-1} for k_1 and k_2, respectively, for the reaction conducted in 4 : 1 THF–H_2O (see ESI†). The result of our stopped-flow experiment concurs with a fast nucleophilic attack of water on the Pd trimer **5**, followed by the slow dissociation to the less stable monomer **7** (Scheme 3), through a series of equilibrating processes. A similar phenomenon was previously observed, where the formation of heterobimetallic complexes from $Pd_3(OAc)_6$ was found to proceed *via* an initial hydrolytic cleavage of the trimeric structure.[50]

3.7 Reduction of Pd(II) to Pd(0)

In previous reports, water was found to accelerate the reduction of tertiary phosphine (PR_3) complexes of palladium(II) acetate to $L_nPd(0)$, but at elevated temperatures.[51,52] Recently, two independent studies of the transmetalation of arylboronic acids to phosphine-ligated palladium complexes were reported,[53,54] which implicated the involvement of a hydroxylpalladium intermediate for the transfer of an aryl group from $ArB(OH)_2$.

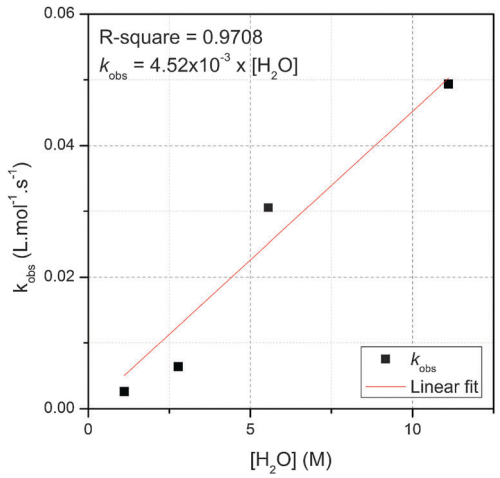

Fig. 8 Reaction rate *vs.* [H_2O] for the dissociation of Pd trimer (**5**).

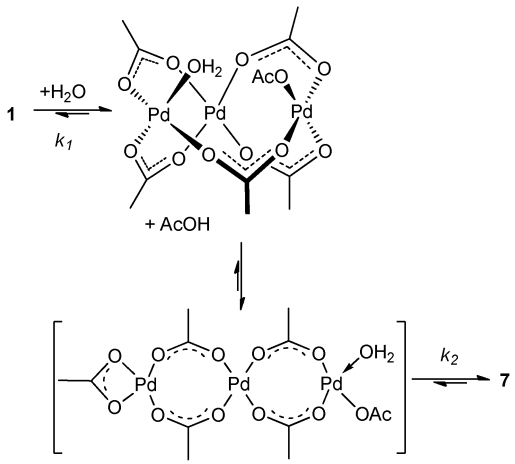

Scheme 3 Reaction between $Pd_3(OAc)_6$ and water.

The formation of Pd(0) species was not observed by the introduction of water, under the reaction conditions adopted by the stopped-flow experiments described above. The addition of two equivalents of arylboronic acid **2**, which contains small traces of water, also did not affect the appearance of the UV spectrum of $Pd_3(OAc)_6$ in anhydrous THF over the timescale of the experiment (75 min, see Fig. S1, ESI†). However, by adding 2 equivalents of arylboronic acid to a solution in 25% H_2O–THF, the formation of biaryl **4** was spontaneously observed, signifying a fast reduction of Pd(II) to Pd(0) *via* double transmetalation and reductive elimination. This was followed by a slow evolution of an absorption peak at *ca.* 450 nm (Fig. 9), which is attributed to the nucleation of Pd(0).[55,56]

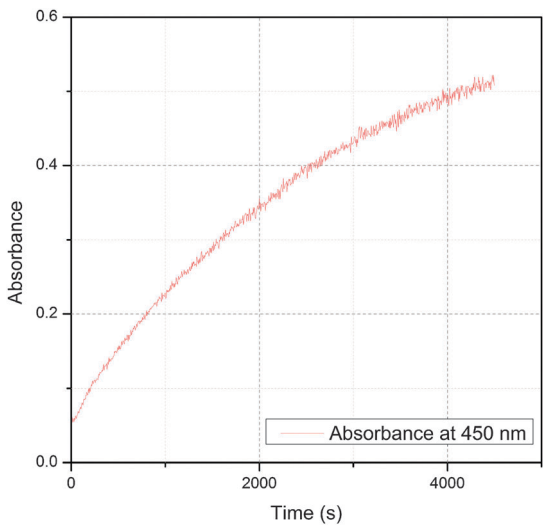

Fig. 9 Evolution of Pd nanoparticles. Conditions: [$Pd(OAc)_2$] = 3.4 mM, 25% H_2O–THF, arylboronic acid **2** (2 equivalents).

Based on these observations, we can deduce that the reduction of palladium(II) acetate is accelerated by water, which first induces a rapid dissociation to monomer **7** (Scheme 4). Water then exchanges with acetate anions to form palladium(II) hydroxide species,[57] which undergoes transmetalation with

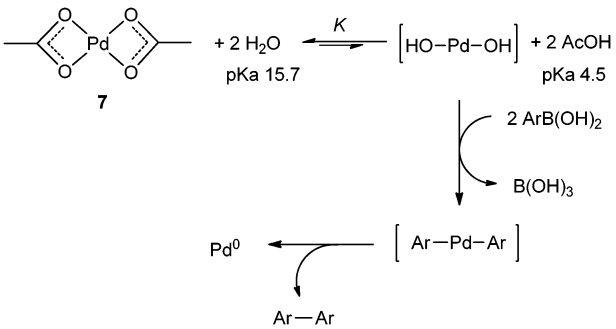

Scheme 4 Reduction of palladium acetate to Pd(0).

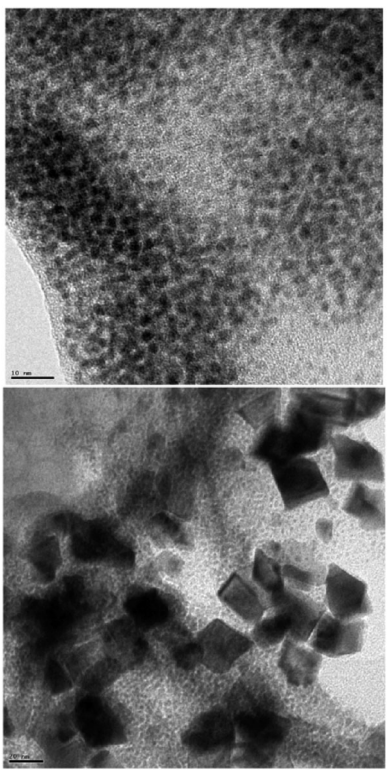

Fig. 10 TEM images of solutions generated from solution of $Pd(OAc)_2$ in arylboronic acid, THF–H_2O (top, scale bar = 10 nm) and arylboronic acid, toluene (bottom, scale bar = 20 nm).

the arylboronic acid to produce palladium(0). The overall process is limited by the highly unfavourable acid–base equilibrium, which is dependent upon the amount of water present and the presence of a base. The reduction of the Pd–OH species by arylboronic acid is extremely rapid (no induction period). At high dilution/low catalytic loading, subsequent formation of Pd···Pd clusters is a slow process.[56,58]

The effect of solvents on the reduction of $Pd(OAc)_2$ can be clearly illustrated by recording TEM images of solutions generated in THF–H_2O or dry toluene in the presence of arylboronic acid (Fig. 10). While the formation of small clusters of colloidal Pd between 2–5 nm is clearly observed in the former, large crystalline $Pd(OAc)_2$ remained largely intact in the anhydrous toluene solution.

4. Conclusions

Our study has unravelled the effect of organic solvent and water on the speciation of $Pd(OAc)_2$ in ligandless SM reactions. Most significantly, water was found to have several roles in the catalyst activation process. The presence of this protic solvent causes a fast dissociation of the $Pd_3(OAc)_6$ trimer, whereupon acid–base equilibrium occurs to generate hydroxopalladium(II) species, which is subsequently reduced by the arylboronic acid to catalytically active Pd(0) species, leading to fast generation of an active catalyst. Conversely, the presence of water maintains the inorganic base in a separate phase, and could create a reservoir for Pd(II) *via* the formation of palladium-phosphate salts (Scheme 5), which may be slowly released into the organic layer over the course of the reaction. The presence of O_2 appears to suppress the catalyst activation process, but also prevents catalyst deactivation, probably by inhibiting the formation of Pd–Pd bonds through the adsorption of O_2.[59,60] Under an N_2 atmosphere, the very fast generation of the catalytically active Pd(0) species is counteracted by an equally rapid Pd aggregation, leading to premature catalyst deactivation (Fig. 2).

Thus, under working catalytic conditions, the presence of water controls the amount of catalytically active Pd(0) released into the reaction mixture, by a series of reversible equilibria. Under SM reaction conditions, the generation of an active catalyst from $Pd(OAc)_2$ is extremely rapid, compared to its transformation by water, arylboronic acid or base (Fig. 3a and b). The presence of O_2 also appears to exert an important effect on catalyst activation (Fig. 2). In both cases, the major catalytic deactivation pathway appears to be the aggregation of Pd to form clusters and nanoparticles.

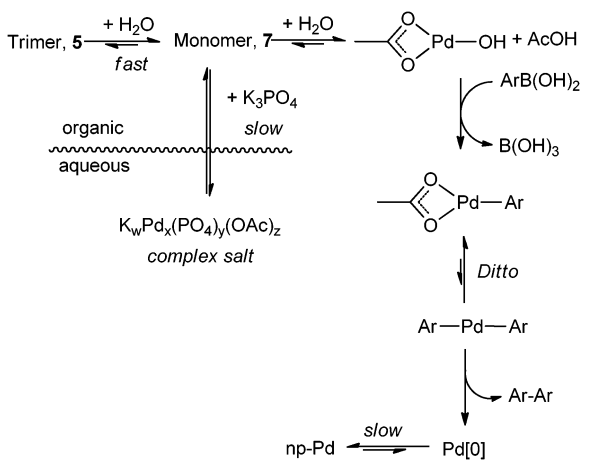

Scheme 5 Summary of interactions of $Pd(OAc)_2$ with H_2O, K_3PO_4 and arylboronic acid.

At this juncture, it is not possible to comment on the nature of the active catalyst in solution, although it is highly likely a mixture of Pd(0) species, ranging from molecular to colloidal species, each with their different reactivities. This inherent complexity makes this a very challenging topic for further research. Nevertheless, work is currently underway to understand this process, as well as to develop effective post-reaction treatment for the removal of palladium residues from the product.[61]

Acknowledgements

LAA is a recipient of a postdoctoral fellowship from Xunta Galicia (Angeles Alvariño program). BNN's postdoctoral fellowship was supported by an EPSRC grant: 'Elucidate and Separate' (ELSEP) (grant number: EP/G070172/1), with further contributions from the Pharmacat Consortium (AstraZeneca, GlaxoSmithKline and Pfizer). We thank Johnson Matthey plc for the provision of Pd salts, and the ESRF for the provision of beam time (project number: CH-2555) and facilities at ID24. We are also grateful to Dr M. Ardakani and Ms E. Ware for help with TEM experiments.

Notes and references

1 J. Sakamoto, M. Rehahn, G. Wegner and A. D. Schluter, *Macromol. Rapid Commun.*, 2009, **30**, 653–687.
2 M. R. Huang, P. Gao and X. G. Li, *Prog. Chem.*, 2010, **22**, 113–118.
3 J. Soloducho, J. Cabaj, K. Idzik, A. Nowakowska-Oleksy, A. Swist and M. Lapkowski, *Curr. Org. Chem.*, 2010, **14**, 1234–1244.
4 W. W. H. Wong, C. Q. Ma, W. Pisula, C. Yan, X. L. Feng, D. J. Jones, K. Mullen, R. A. J. Janssen, P. Bauerle and A. B. Holmes, *Chem. Mater.*, 2010, **22**, 457–466.
5 O. Baudoin, M. Cesario, D. Guenard and F. Gueritte, *J. Org. Chem.*, 2002, **67**, 1199–1207.
6 U. V. Mentzel, D. Tanner and J. E. Tonder, *J. Org. Chem.*, 2006, **71**, 5807–5810.
7 S. S. Kulkarni and A. H. Newman, *Bioorg. Med. Chem. Lett.*, 2007, **17**, 2074–2079.
8 E. Perissutti, F. Frecentese, A. Lavecchia, F. Fiorino, B. Severino, F. De Angelis, V. Santagada and G. Caliendo, *Tetrahedron*, 2007, **63**, 12779–12785.
9 R. Severinsen, G. T. Bourne, T. T. Tran, M. Ankersen, M. Begtrup and M. L. Smythe, *J. Comb. Chem.*, 2008, **10**, 557–566.
10 H. Fuwa, A. Saito, S. Naito, K. Konoki, M. Yotsu-Yamashita and M. Sasaki, *Chem.–Eur. J.*, 2009, **15**, 12807–12818.
11 Y. Nakama, O. Yoshida, M. Yoda, K. Araki, Y. Sawada, J. Nakamura, S. Xu, K. Miura, H. Maki and H. Arimoto, *J. Med. Chem.*, 2010, **53**, 2528–2533.
12 U. Christmann and R. Vilar, *Angew. Chem., Int. Ed.*, 2005, **44**, 366–374.
13 N. Marion and S. P. Nolan, *Acc. Chem. Res.*, 2008, **41**, 1440–1449.
14 V. F. Slagt, A. H. M. de Vries, J. G. de Vries and R. M. Kellogg, *Org. Process Res. Dev.*, 2010, **14**, 30–47.
15 C. Torborg and M. Beller, *Adv. Synth. Catal.*, 2009, **351**, 3027–3043.

16 A. Arcadi, G. Cerichelli, M. Chiarini, M. Correa and D. Zorzan, *Eur. J. Org. Chem.*, 2003, 4080–4086.
17 Y. J. Deng, L. Z. Gong, A. Q. Mi, H. Liu and Y. Z. Jiang, *Synthesis*, 2003, 337–339.
18 B. W. Xin, Y. H. Zhang, L. F. Liu and Y. G. Wang, *Synlett*, 2005, 3083–3086.
19 K. Sawai, R. Tatumi, T. Nakahodo and H. Fujihara, *Angew. Chem., Int. Ed.*, 2008, **47**, 6917–6919.
20 B. W. Xin, *J. Chem. Res.*, 2008, 412–415.
21 A. Del Zotto, F. Amoroso, W. Baratta and P. Rigo, *Eur. J. Org. Chem.*, 2009, 110–116.
22 F. Durap, M. Rakap, M. Aydemir and S. Ozkar, *Appl. Catal., A*, 2010, **382**, 339–344.
23 Y. Y. Peng, J. B. Liu, X. L. Lei and Z. L. Yin, *Green Chem.*, 2010, **12**, 1072–1075.
24 C. Li, X. Q. Li and C. Zhang, *J. Chem. Res*, 2008, 525–527.
25 L. F. Liu, Y. H. Zhang and Y. G. Wang, *J. Org. Chem.*, 2005, **70**, 6122–6125.
26 R. Tatumi, T. Akita and H. Fujihara, *Chem. Commun.*, 2006, 3349–3351.
27 W. Han, C. Liu and Z. L. Jin, *Org. Lett.*, 2007, **9**, 4005–4007.
28 W. Han, C. Liu and Z. L. Jin, *Adv. Synth. Catal.*, 2008, **350**, 501–508.
29 J. M. A. Miguez, L. A. Adrio, A. Sousa-Pedrares, J. M. Vila and K. K. Hii, *J. Org. Chem.*, 2007, **72**, 7771–7774.
30 C. Liu, Q. Ni, P. Hu and J. Qiu, *Org. Biomol. Chem.*, 2011, **9**, 1054–1060.
31 J. C. Labiche, O. Mathon, S. Pascarelli, M. A. Newton, G. Guilera-Ferré, C. Curfs, G. Vaughan, A. Homs and D. F. Carreiras, *Rev. Sci. Instrum.*, 2007, **78**, 091301.
32 (*a*) K. V. Klementiev, VIPER for Windows, freeware; (*b*) K. V. Klementiev, *J. Phys. D: Appl. Phys.*, 2001, **34**, 209.
33 Z. Xu, J. C. Mao and Y. W. Zhang, *Catal. Commun.*, 2008, **9**, 97–100.
34 $<4\%$ at 1 mol% catalyst loading, and not detected ($<0.1\%$) at 0.05 mol%.
35 Homocoupled product **4** was not observed under these reaction conditions.
36 Water is necessary to ensure solubility of the inorganic base. Also, arylboronic acid dehydrates to arylboroxine under anhydrous conditions.
37 Q. Yao, E. P. Kinney and Z. Yang, *J. Org. Chem.*, 2003, **68**, 7528–7531.
38 Palladium(II) acetate is soluble in THF but practically insoluble in water.
39 A. El Maadi, J. Bennazha, J. M. Réau, A. Boukhari and E. M. Holt, *Mater. Res. Bull.*, 2003, **38**, 865–874.
40 Elemental analysis by ICP and combustion analysis: Pd, 57.69; P, 4.24; C, 1.71 and H, 3.99%.
41 A. C. Skapski and M. L. Smart, *J. Chem. Soc. D*, 1970, 658.
42 S. D. Kirik, R. F. Mulagaleev and A. I. Blokhin, *Acta Crystallogr., Sect. C: Cryst. Struct. Commun.*, 2004, **60**, M449–M450.
43 T. A. Stephenson, S. M. Morehouse, A. R. Powell, J. P. Heffer and G. Wilkinson, *J. Chem. Soc.*, 1965, 3632–3640.
44 R. N. Pandey and P. M. Henry, *Can. J. Chem.*, 1974, **52**, 1241–1247.
45 E. S. Stoyanov, *J. Struct. Chem.*, 2000, **41**, 440–445.
46 J. Evans, L. O'Neill, V. L. Kambhampati, G. Rayner, S. Turin, A. Genge, A. J. Dent and T. Neisius, *J. Chem. Soc., Dalton Trans.*, 2002, 2207–2212.
47 V. I. Bakhmutov, J. F. Berry, F. A. Cotton, S. Ibragimov and C. A. Murillo, *Dalton Trans.*, 2005, 1989–1992.
48 J. A. Ruddick and W. B. Bunger, in *"Techniques of Chemistry"*, ed. A. Weissberger, Wiley-Interscience, New York, 1986.
49 Chosen for its low polarity, miscibility with water and the ability to dissolve arylboronic acid.
50 N. S. Akhmadullina, N. V. Cherkashina, N. Y. Kozitsyna, I. P. Stolarov, E. V. Perova, A. E. Gekhman, S. E. Nefedov, M. N. Vargaftik and Moiseev, II, *Inorg. Chim. Acta*, 2009, **362**, 1943–1951.
51 F. Ozawa, A. Kubo and T. Hayashi, *Chem. Lett.*, 1992, 2177–2180.
52 B. Fors and B. P. Fors, *Org. Lett.*, 2008, **10**, 3505.
53 C. Amatore, A. Jutand and G. Le Duc, *Chem.–Eur. J.*, 2011, **17**, 2492–2503.
54 B. P. Carrow and J. F. Hartwig, *J. Am. Chem. Soc.*, 2011, **133**, 2116–2119.
55 J. Wang, H. F. M. Boelens, M. B. Thathagar and G. Rothenberg, *ChemPhysChem*, 2004, **5**, 93–98.
56 A. V. Gaikwad and G. Rothenberg, *Phys. Chem. Chem. Phys.*, 2006, **8**, 3669–3675.
57 A. Kitamura and M. Yui, *J. Nucl. Sci. Technol.*, 2010, **47**, 760–770.
58 E. E. Finney and R. G. Finke, *J. Colloid Interface Sci.*, 2008, **317**, 351–374.
59 A. N. Salanov, A. I. Titkov and V. N. Bibin, *Kinet. Catal.*, 2006, **47**, 430–436.
60 A. N. Salanov and E. A. Suprun, *Kinet. Catal.*, 2009, **50**, 31–39.
61 S. Malladi, B. N. Nguyen, K. K. Hii and A. G. Livingston, unpublished results.